Hindawi
Journal of Nanomaterials
Volume 2018, Article ID 5470814, 11 pages
https://doi.org/10.1155/2018/5470814

Research Article

Copper-Doped Nano Laponite Coating on Poly(butylene Succinate) Scaffold with Antibacterial Properties and Cytocompatibility for Biomedical Application

Xiaoming Tang,[1] Jian Dai,[1] Hailang Sun,[1] Saha Nabanita,[2] Saha Petr,[2] Liangchen Tang,[3] Qilin Cheng,[3] Deqiang Wang,[3] and Jie Wei[3]

[1]*Department of Orthopedics, Huai'an First People's Hospital, Nanjing Medical University, Huai'an, 223001 Jiangsu Province, China*
[2]*Centre of Polymer Systems, University Institute, Tomas Bata University in Zlin, Tr T Bati 5678, Zlin 76001 Zlin, Czech Republic*
[3]*Key Laboratory for Ultrafine Materials of Ministry of Education, East China University of Science and Technology, Shanghai 200237, China*

Correspondence should be addressed to Hailang Sun; 3132793530@qq.com

Received 20 June 2018; Revised 25 September 2018; Accepted 17 October 2018; Published 19 December 2018

Academic Editor: Angelo Taglietti

An ideal artificial bone will likely be multifunctional, combining different technologies to simultaneously promote bone regeneration while inhibiting microbial infection. In this study, copper- (Cu-) doped nano laponite (cnLAP) was prepared by a cation-exchanged method, and the cnLAP coating on poly(butylene succinate) (PBSu) scaffold was fabricated by poly(dopamine) modification. The results showed that incorporation of Cu ions into nano laponite (nLAP) did not have obvious effects on the morphology and surface area of cnLAP (compared with nLAP), which could be coated easily on macroporous PBSu scaffolds. In addition, the cnLAP-coated PBSu scaffolds could inhibit the growth of both *Escherichia coli (E. coli)* and *Staphylococcus aureus (S. aureus)*, indicating good antibacterial activity. Moreover, the cnLAP-coated PBSu scaffolds significantly promoted proliferation and improved alkaline phosphatase (ALP) activity of bone mesenchymal stem cells (BMSCs) compared with PBSu scaffolds. Furthermore, no obvious differences in cell responses to cnLAP- and nLAP-coated PBSu scaffolds were found, indicating that incorporation of Cu into nLAP had no negative effects on its cytocompatibility. The results suggested that the cnLAP-coated PBSu scaffolds exhibited excellent cytocompatibility and antimicrobial activity, which might offer promising opportunities for promoting bone regeneration and prevention of infectious from bacteria and effective treatment of bone defects.

1. Introduction

As one of synthetically biodegradable polymers, poly(butylene succinate) (PBSu) has been applied in tissue engineering and regeneration medicine because of its excellent biocompatibility, good processing ability, nontoxic degradable products, etc. [1, 2]. However, as a biomaterial for bone implanted scaffold applications, PBSu still has some disadvantages; for example, PBSu is a hydrophobic polymer, which may not be in favor of cell attachment onto its surface or cell infiltration into its porous structure [3]. In addition, the biological inertness of PBSu may hinder the osteogenesis and new bone tissue growth into the PBSu scaffold [4]. Therefore, as a scaffold for bone regeneration, it is necessary to improve the biological performances (e.g., bioactivity/biocompatibility) of PBSu scaffolds.

Nano laponite (nLAP) is a synthetic silicate nanomaterial composed of nanoscale crystals, which has recently been paid more attention to be developed as a new functional material in nanomedicine, namely, for the diagnosis and treatment of diseases, as well as for regenerative medicine and tissue engineering [5, 6]. nLAP can be readily degradable in the physiological environment giving rise to nontoxic and even bioactive products [7]. The discovery that nLAP is bioactive, itself capable of promoting osteogenic differentiation of human mesenchymal stem cells (hMSCs), resulted in the

increase in research interest on its application for bone tissue regeneration [8, 9]. Studies have shown that nLAP could induce the osteogenic differentiation of MC3T3-E1 cells by enhancing alkaline phosphatase (ALP) activity, runt-related transcription factor 2 (RUNX2) transcript upregulation, and bone-related matrix protein deposition (e.g., osteocalcin and osteopontin), followed by matrix mineralization [10, 11]. nLAP presents Mg and Si ions in the octahedral sites and Li ions in minor amount, and Na ions in the interlayer domain, which can form transparent colloidal suspensions in water [12]. Moreover, when nLAP crystals are dispersed in water, the sodium ions in negatively charged silicate layers can release and readily exchange for other ions (such as Ca and Cu ions) (cation-exchanged method) due to its high specific surface area with good adsorptive capacity [13].

With the rapid development of the biomaterial industry, biomaterial centred infections have become a very knotty clinical problem, and infection is one of the primary causes of failure of orthopedic implant for bone repair [14, 15]. Generally, resistance to bacterial infection would be a very desirable property of bone implanted materials. Copper (Cu) has excellent antibacterial properties against numerous bacteria, and incorporation of copper into medical devices to enhance their antibacterial activity has drawn considerable attention [16, 17]. It was reported that the minimum inhibitory concentrations of Cu ions on *E. coli* and *S. aureus* were 100 mg/L [18]. Previous studies showed that the trace amounts of Cu (50 mM) promoted the osteogenic ability of marrow stem cells, and Cu-doped calcium phosphate cements enhanced the activity and proliferation of osteoblastic cells [19, 20]. Clearly, incorporation of Cu ions into biomaterials is a promising alternative to stimulate cellular activity for promoting bone regeneration. An ideal artificial bone will likely be multifunctional, combining different technologies to simultaneously promote bone regeneration while inhibiting microbial infection [21]. Therefore, in this study, the Cu-doped nLAP (cnLAP) was fabricated by the cation-exchanged method, and cnLAP coating on macroporous PBSu scaffold was prepared by poly(dopamine) modification. Moreover, the antimicrobial property and BMSC responses to the cnLAP-coated PBSu scaffold were evaluated in this study. The objective of this study is to prepare bioactive coating on PBSu scaffolds with antimicrobial activity and good biocompatibility for bone repair.

2. Materials and Methods

2.1. Preparation and Characterization of cnLAP and PBSu Scaffold. To prepare the Cu-exchanged nLAP (cnLAP), 0.2 g nLAP powders (Altana, Germany) were firstly dispersed in 100 mL deionized water to obtain the suspension, and 0.03 g cupric sulfate ($CuSO_4$, Shanghai Lingfeng Chemical Reagent Co. Ltd., China) was then added into the suspension with stirring for 4 h at 37°C. The resulting suspension was filtered and washed with deionized water for 3 times to remove the residual $CuSO_4$. The products were collected and dried at 55°C for 48 h to obtain the cnLAPc powders. The surface morphology and microstructure of both obtained cnLAP and nLAP were characterized by using transmission electron microscopy (TEM, JEM-2100, JEOL, Japan). In addition, the specific surface areas of both cnLAP and nLAP powder were determined by using TriStar II 3020 (Micromeritics, USA) to obtain the nitrogen adsorption-desorption isotherms and calculated by Brunauer-Emmett-Teller (BET). Moreover, the particle size distribution (PSD) of both cnLAP and nLAP powder was tested by dynamic light scattering (DLS).

The PBSu scaffolds were firstly fabricated by using a solvent casting-particulate leaching method using NaCl as the porogen. Briefly, 1 g PBSu (Anqing Hexing Chemical Co. Ltd., China) particles were dissolved into 10 mL chloroform (Shanghai Lingfeng Chemical Reagent Co. Ltd., China) for 10 min to form the PBSu slurry. Then, 10 g sodium chloride (NaCl) particles (size of around 300~500 μm) were added into the above slurry with vigorous stirring for 1 h, and the PBSu/NaCl paste was obtained. The resulting mixture paste was then placed into the stainless steel molds ($\Phi 12 \times 2$ mm) and compressed by a compressing machine (YP-15T, Jinfulun Technology Co. Ltd., China) under pressure of 4 MPa. The samples were collected and immersed into deionized water for 48 h to remove the NaCl and air-dried at 60°C to get the final PBSu scaffolds.

2.2. Preparation and Characterization of cnLAP Coating on PBSu Scaffolds. The coating of cnLAP and nLAP (as a control) onto the PBSu scaffolds was conducted via direct immersion coating. Briefly, 2 mg/mL dopamine hydrochloride solution (Sigma-Aldrich, USA) was dissolved in 50 mM Tris-HCl solution (pH 8.5) at 25°C. Then, the PBSu scaffolds were immersed into 10 mL dopamine solution for 12 h with continuous string, followed by several rinses with deionized water and drying to obtain the PBSu scaffolds with PDA coating. The PBSu scaffolds with PDA coatings were immersed in cnLAP for 24 h at 25°C to get PBSu scaffolds with cnLAP coating (cnLBC). In addition, the PBSu scaffolds with PDA coatings were immersed in nLAP for 24 h at 25°C to get PBSu scaffolds with nLAP coating (nLBC, as a control),which were used as controls. The scaffolds (PBSu, nLBC, and cnLBC) were characterized by using a scanning electron microscope (SEM), energy-dispersive spectrometer (EDS), Fourier transform infrared spectrometer (FTIR, Nicolet 6700, Nicolet, USA), rotating anode X-ray powder diffractometer (XRD, D/MAX 2550 VB/PC, Rigaku Co., Japan), and X-ray photoelectron spectroscope (XPS, ESCALAB 250Xi, Thermo Scientific, USA).

2.3. Assessment of Antibacterial Activity of Scaffolds. The antibacterial activity of the PBSu, nLBC, and cnLBC scaffolds ($\Phi 12 \times 2$ mm) were determined by bacteria counting using *Escherichia coli* (*E. coli*, ATCC 25922) and *Staphylococcus aureus* (*S. aureus*, ATCC 25923). All samples were sterilized by ethylene oxide prior to the following process. 60 μL of bacteria solution (10^7 CFU/mL) was added on the sample surfaces in 24-well plates. After 24 h of cocultivation at 37°C, the samples were transferred into a 10 mL sterilized centrifuge tube, and 4 mL of sterilized physiological saline was added into the tube. After that, the tube was vigorously agitated to detach the bacteria from samples, and the resulting solution was collected and diluted 10, 100, and 1000 times

with sterilized physiological saline. Afterwards, 100 μL of the diluted solution was introduced to Luria-Bertani agars (*E. coli*) and tryptic soy broth agars (*S. aureus*) and cultured for 24 hours under the culturing condition of 37°C. In addition, 100 μL of vancomycin water solution was used as a positive control in this study. The active bacteria were counted according to the National Standard of China GB/T 4789.2 protocol, and the percent reductions of bacteria were calculated as follows:

$$\text{Percent reduction}\,(\%) = \frac{(A-B)}{A} \times 100\%, \quad (1)$$

where A is the average number of bacteria on the PBSu scaffolds (CFU/sample) and B is the average number of bacteria on nLBC and cnLBC scaffolds (CFU/samples).

2.4. In Vitro Cytocompatibility

2.4.1. Cell Culture. Cell experiments were performed using mouse bone marrow stromal cells (BMSCs) in this study, which were purchased from Shanghai Institutes for Biological Science, Chinese Academy of Science (Shanghai, China). BMSCs were cultured in DMEM (Dulbecco's modified Eagle's medium, HyClone, China) supplemented with 10% fetal calf serum (FBS, 10%, Gibco, Thermo Fisher Scientific, USA), penicillin (100 U/mL), and streptomycin (100 μg/mL) under an atmosphere of 100% humidity and 5% CO_2 at 37°C. The culture medium was exchanged every 3 d.

2.4.2. Cell Morphology and Proliferation. For the observation of cell morphology cultured on PBSu, nLBC, and cnLBC scaffolds ($\Phi 12 \times 2$ mm) at day 3, the samples were rinsed twice with phosphate-buffered saline (PBS) and fixed in 0.25% glutaraldehyde for 2 h. Afterwards, the cell-seeded samples (with density of 2×10^4 cells/well) were stained with 4′,6-diamidino-2-phenylindole (Sigma, DAPI) and fluorescein isothiocyanate (Sigma, FITC) for 40 min and 5 min, respectively. The morphology of the cells on different scaffolds was observed by confocal laser scanning microscopy (CLSM, Nikon A1R, Nikon, Japan).

The cell proliferation on PBSu, nLBC, and cnLBC scaffolds ($\Phi 12 \times 2$ mm) was assessed with Cell Counting Kit-8 (CCK-8, Dojindo Molecular Technologies Inc., Japan). Briefly, at each cultivation time point (day 1, 3, and 5), the culture medium was removed and the samples were washed with PBS solution for 3 times. Then, the cells on the sample surface of each well were incubated with cell medium (400 μL) containing CCK-8 solution (40 μL) for 6 hours. The optical density (OD) at 450 nm of solution was measured by a microplate reader (Synergy HT, USA).

2.4.3. Alkaline Phosphatase (ALP) Activity. To evaluate the ALP activity of the cells on the samples, the PBSu, nLBC, and cnLBC scaffolds ($\Phi 12 \times 2$ mm) were cultured with BMSC cells with density of 2×10^4 cells/well in 24-well culture plates for 7, 10, and 14 d. Then, the Nonidet P40 solution (NP-40, 1%, 200 μL) was added and incubated at 37°C for 1 h. The cell lysate was obtained and centrifuged. 50 μL supernatant was added to a new 96-well culture plate, and 50 μL p-nitrophenylphosphate (2 mg/mL, Sangon, Shanghai, China) solution combined with glycine (0.1 mol/L) and $MgCl_2 \cdot 6H_2O$ (1 mmol/L) was added for another 30 min of incubation at 37°C. Then, 100 μL NaOH (0.1 mol/L) solution was added to stop the reaction, and a microplate reader was used to measure the absorbance of ALP at a wavelength of 405 nm. The total protein content in the cell lysate was determined using the bicinchoninic acid (BCA) method in aliquots of the same samples with the Pierce protein assay kit (Pierce Biotechnology Inc., USA) and read at 562 nm and calculated according to a series of albumin (bovine serum albumin) standards. The ALP levels were normalized to the total protein content. All experiments were performed in triplicate.

2.4.4. Ions Release from Scaffolds in Cell Culture Medium. To investigate the changes of ion concentrations in cell culture medium during the culture of BMSCs with PBSu, nLBC, and cnLBC scaffolds ($\Phi 12 \times 2$ mm), the cell culture medium for the cell proliferation test was collected at days 1, 3, 5, 7, 10, and 14, and the concentrations of Mg, Li, and Cu ions from the scaffolds were detected by ICP-AES (IRIS 1000, Thermo Elemental, USA). The ion concentrations in DMEM without samples were also measured as the negative group.

2.4.5. Statistical Analysis. The data were analyzed using Origin 8.0 and are presented as the mean ± standard deviation with $n = 3$. Statistical difference was evaluated by variance analysis (ANOVA one-way, Origin 8.0). A value of $p < 0.05$ was regarded as statistically significant.

3. Results

3.1. Characterization of cnLAP. Figures 1(a) and 1(b) show the TEM micrographs of morphology of nLAP and cnLAP. It was found that both nLAP and cnLAP were of lamellar-like structure with particle sizes of 30-40 nm. After Cu ions substituted for Na ions in nLAP, no significant differences in morphology and particle size between nLAP and cnLAP were observed. Figure 1(c) shows the specific surface area of both nLAP and cnLAP, and the surface areas of nLAP and cnLAP were 378 m^2/g and 365 m^2/g, respectively. The results revealed that incorporation of Cu into nLAP had no significant effects on the surface areas of cnLAP compared with nLPAP. Figures 1(d) and 1(e) show the particle size distribution (PSD) of both cnLAP and nLAP. It can be seen that most of the particle sizes of both cnLAP and nLAP were 30-40 nm, which were consistent well with the TEM micrographs.

3.2. Characterization of cnLAP Coating on PBSu Scaffolds. Figures 2(a)–2(c) show the SEM micrographs of surface morphology of PBSu, nLBC, and cnLBC scaffolds. The macropore size of scaffolds was found to be in the range of 200-500 μm, which were consistent with the size of NaCl particles (used to prepare the scaffolds). In the high magnification of SEM micrographs as shown in Figures 2(d)–2(f), many homogeneous flake-like substances were found on the surface of the nLBC and cnLBC scaffolds (nLAP and cnLAP coating) compared with the PBSu scaffold without coating. Moreover, the images of EDS mapping (scaffold

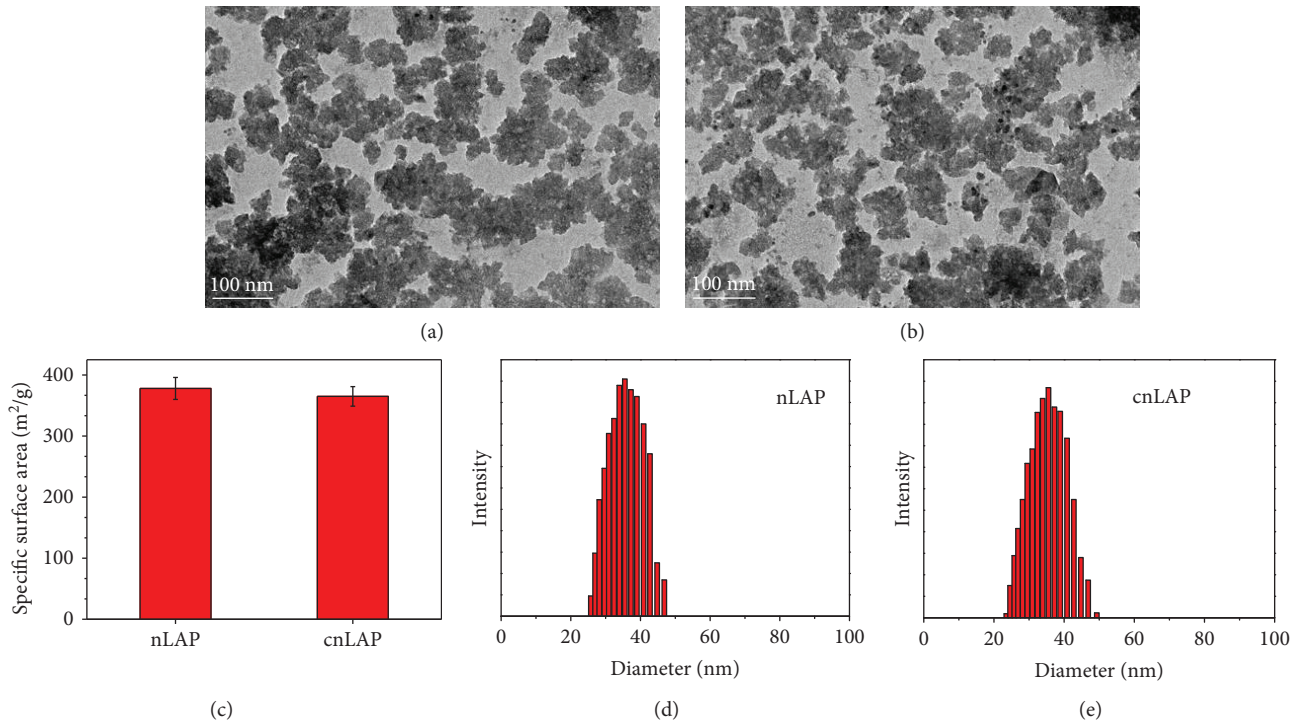

Figure 1: Transmission electron microscopy (TEM) micrographs of morphology of nano laponite (nLAP, a) and Cu-exchanged nLAP (cnLAP, b), specific surface area (c), and dynamic light scattering (DLS) analysis (d, e) of nLAP and cnLAP.

surface) showed that only the C element (no Si and Cu) was distributed on PBSu scaffolds (Figure 2(g)), and the C and Si elements (no Cu) were distributed on nLBC scaffolds (Figure 2(h)). However, the C, Si, and Cu elements were distributed on cnLBC scaffolds (Figure 2(i)).

Figure 3(a) shows the IR of nLAP and cnLAP, and PBSu, nLBC, and cnLBC scaffolds. For nLAP and cnLAP, the peak at 1006 cm^{-1} corresponded to Si-O-Si asymmetric stretching, and 1637 cm^{-1} and 3426 cm^{-1} corresponded to structural hydroxyls and absorbed water. No obvious difference in IR was found between nLAP and cnLAP. For PBSu, the peaks at 1720 cm^{-1} and 3430 cm^{-1} corresponded to the C=O stretching and free O-H groups. For nLBC and cnLBC scaffolds, the peaks at 1006 cm^{-1} and 1637 cm^{-1} and 3426 cm^{-1} were attributed to nLAP and cnLAP, indicating that both nLAP and cnLAP were coated on PBSu scaffolds.

Figure 3(b) shows the XRD patterns of nLAP and cnLAP and PBSu, nLBC, and cnLBC scaffolds. The characteristic peaks at $2\theta = 20°$, 28°, 35°, and 61° corresponded to nLAP and cnLAP. No obvious difference in XRD was found between nLAP and cnLAP. The characteristic peaks at $2\theta = 19.5°$, 22.8°, and 28.2° corresponded to PBSu. Meanwhile, it was found that both nLBC and cnLBC scaffolds contained the characteristic peaks of both PBSu and cnLAP (nLAP).

Figure 4 shows XPS spectra of PBSu, nLBC, and cnLBC scaffolds. The PBSu scaffold only contained C and O elements, which appeared at 285 and 533 eV, respectively. After coating with nLAP/cnLAP, the peaks for Mg, Na, and Si (Mg1s, Na1s, and Si2p) were observed on both nLBC and cnLBC scaffolds, whereas no peak for Mg1s, Na1s, and Si2p were found on PBSu. The Mg, Na, and Si elements on both nLBC and cnLBC scaffolds appeared at 1305, 1074, and 102 eV, respectively. Furthermore, for cnLAP coating, the Cu element was found on the cnLBC scaffold surface, indicating that the Cu element was incorporated into the cnLAP coating.

3.3. Antibacterial Properties of Scaffolds. Figure 5 shows the digital photographs of bacteria of the *E. coli* and *S. aureus* colonies after incubation with PBSu, nLBC, and cnLBC scaffolds for 24 hours (including a positive control, vancomycin). No bacteria colonies were found for vancomycin, showing good antimicrobial activity. In addition, few bacteria colonies were found for cnLBC, indicating that cnLBC scaffolds possessed antimicrobial activity, which could inhibit the growth of both *E. coli* and *S. aureus*. However, a large number of bacteria were found for PBSu and nLBC scaffolds, implying no antimicrobial activity of PBSu and nLBC scaffolds, which could not inhibit the growth of both *E. coli* and *S. aureus*.

Figure 6 shows the percent reductions of both *E. coli* and *S. aureus* after being cocultured with PBSu, nLBC, and cnLBC scaffolds for 24 h. The percent reduction of *E. coli* was 90.7% and that of *S. aureus* was 92.3% for cnLBC, indicating good antimicrobial activity (percent reduction for vancomycin on two bacteria of 100%). However, the percent reduction of *E. coli* was 0 and *S. aureus* was 0 for both nLBC and PBSu, indicating no antimicrobial activity.

3.4. Cell Adhesion and Morphology on Scaffolds. Figure 7 shows the CLSM images of morphology of BMSCs stained on PBSu, nLBC, and cnLBC scaffolds. It can be seen that only

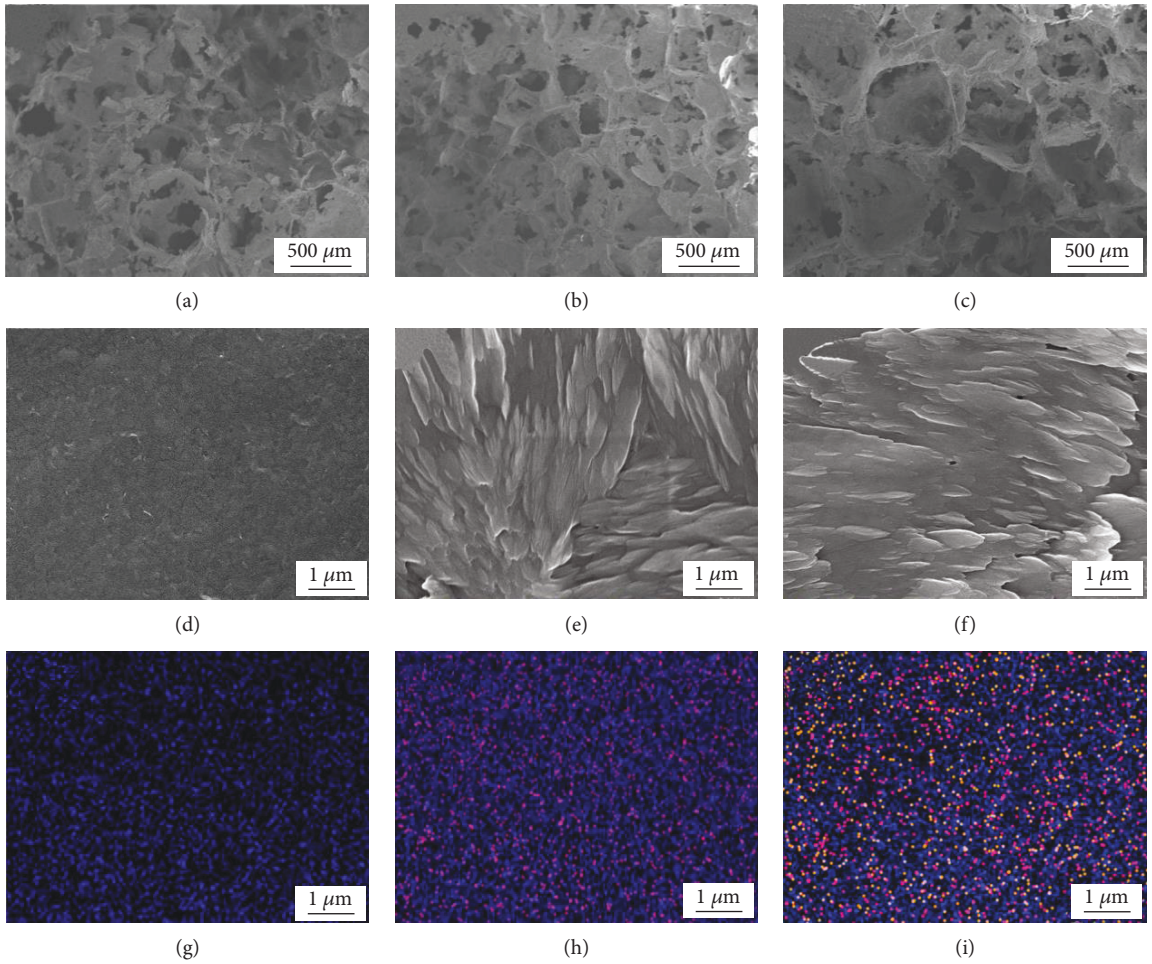

Figure 2: Scanning electron microscope (SEM) micrographs of surface morphology of PBSu (a, d), nLBC (b, e), and cnLBC (c, f) scaffolds, and images of energy-dispersive spectrometer (EDS) mapping of the scaffolds; blue dots represent carbon-C (in g), purple dots represent silicon-Si (in h), and yellow dots represent Cu (in f).

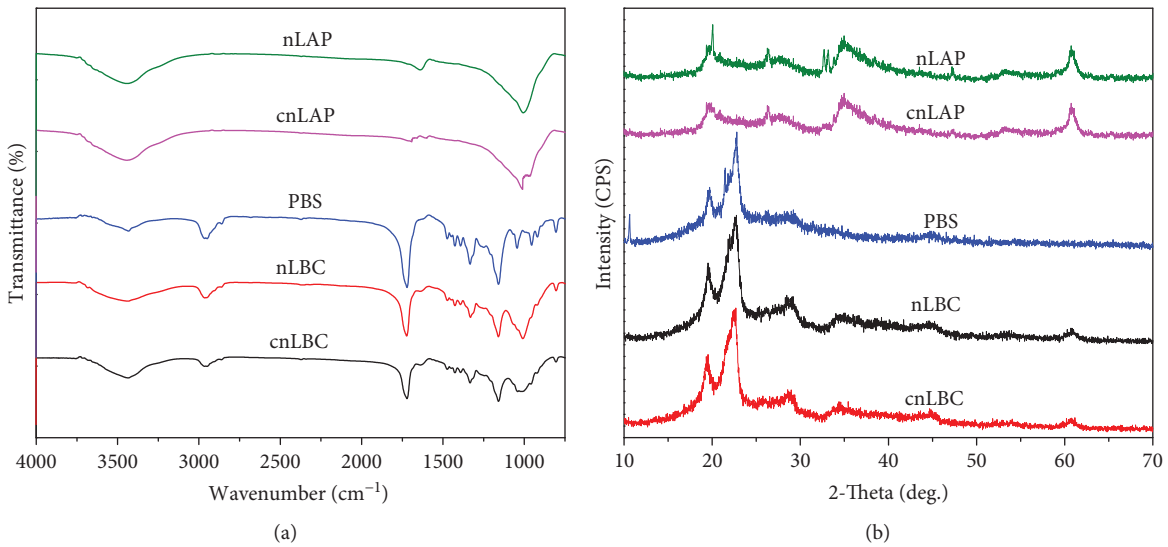

Figure 3: Fourier transform infrared spectrometry (FTIR, a) and X-ray powder diffractometer (XRD, b) patterns of nLAP and cnLAP, and poly(butylene succinate) (PBSu), nLAP coating (nLBC), and cnLAP coating (cnLBC) scaffolds.

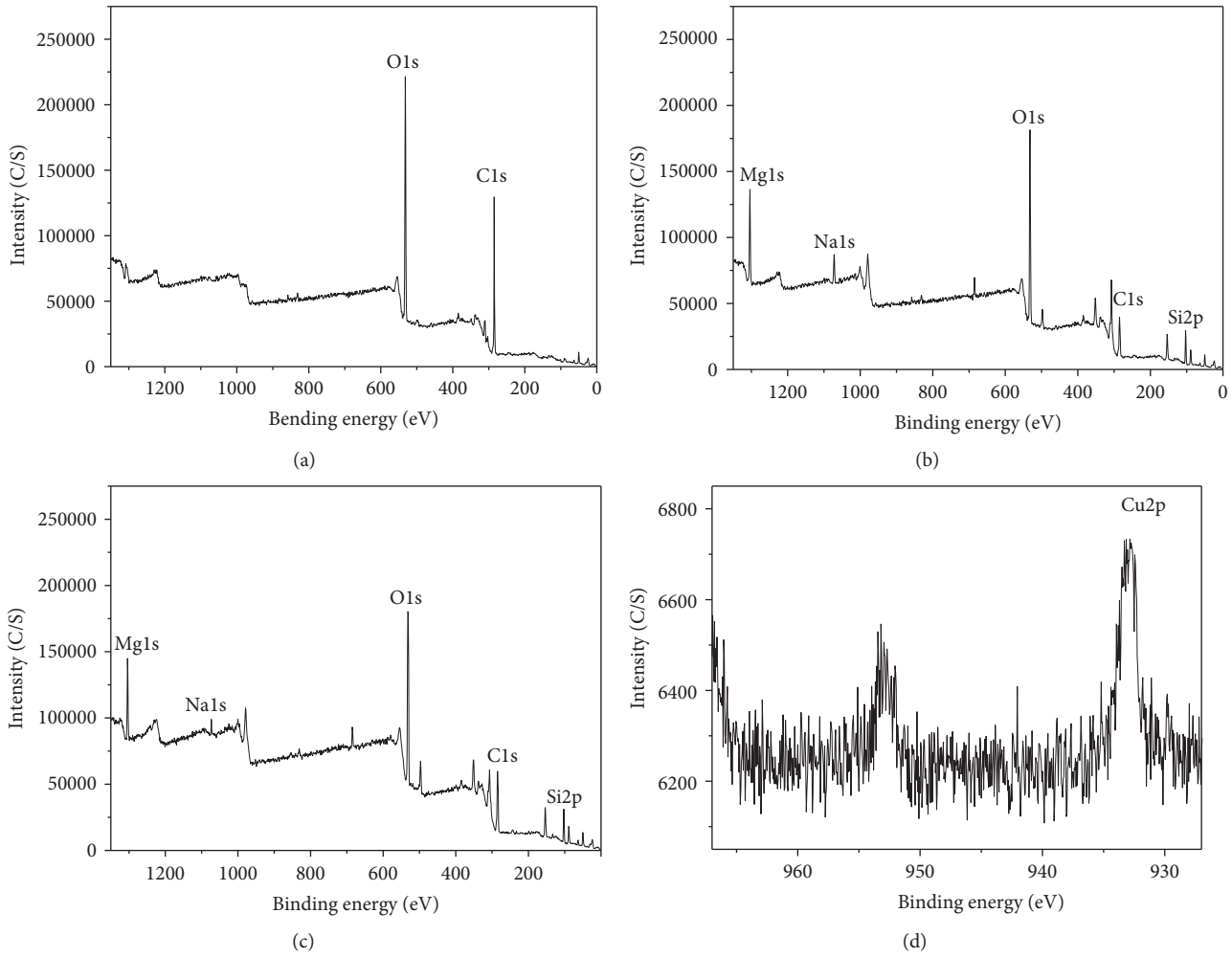

Figure 4: X-ray photoelectron spectroscopy (XPS) spectra of PBSu (a), nLBC (b), and cnLBC (c) scaffolds, and enlarged XPS spectra (d) between 967 and 927 eV of cnLBC.

a few cells attached on PBSu scaffolds (Figures 7(a) and 7(d)). However, a great number of cells attached on both nLBC (Figures 7(b) and 7(e)) and cnLBC (Figures 7(c) and 7(f)) scaffolds after 1 and 3 days of culturing. The cell spread morphology and amount of cells improved with time. In addition, there was no significant difference in cell morphology and amount of BMSCs cultured on nLBC and cnLBC scaffolds.

3.5. Proliferation and ALP Activity of Cells on Scaffolds. Figure 8(a) shows the OD values of the BMSCs on the PBSu, nLBC, and cnLBC scaffolds at different time points. The OD values of the cells on PBSu, nLBC, and cnLBC scaffolds increased with time, indicating that the cells could proliferate on these scaffolds. The OD values of the cells cultured on both nLBC and cnLBC were significantly higher than PBSu scaffolds at 1, 3, and 5 days, indicating that coatings of nLAP and cnLAP on PBSu improved the cell proliferation. Moreover, no significant differences in OD values were found on both nLBC and cnLBC scaffolds. The results revealed that both nLBC and cnLBC scaffolds significantly promoted cell proliferation as compared with PBSu scaffold ($p < 0.05$).

Figure 8(b) shows the ALP activity of BMSCs on the PBSu, nLBC, and cnLBC scaffolds at different time points. At 7 d, no significant differences in ALP activity of the cells were found on PBSu, nLBC, and cnLBC scaffolds. However, at both 10 and 14 d, ALP activity of the cells on both nLBC and cnLBC scaffolds were obviously higher than that of the PBSu scaffold ($p < 0.05$). Furthermore, no significant difference in ALP activity was found between nLBC and cnLBC scaffolds.

3.6. Ions Release from Scaffolds into Cell Culture Medium. Figure 9 shows the change in concentrations of Mg, Li, Si, and Cu ions in the cell culture medium with time after the BMSCs were cultured on PBSu, nLBC, and cnLBC scaffolds. The concentrations of Mg, Si, and Li ions in the cell culture medium for both nLBC and cnLBC scaffolds gradually increased with time because these ions were gradually released from the two scaffolds into the medium (dissolution of cnLAP and nLAP). Moreover, the Cu ions were found to release from the cnLBC scaffold into the medium. However, No these ions were found to release from PBSu scaffold into medium.

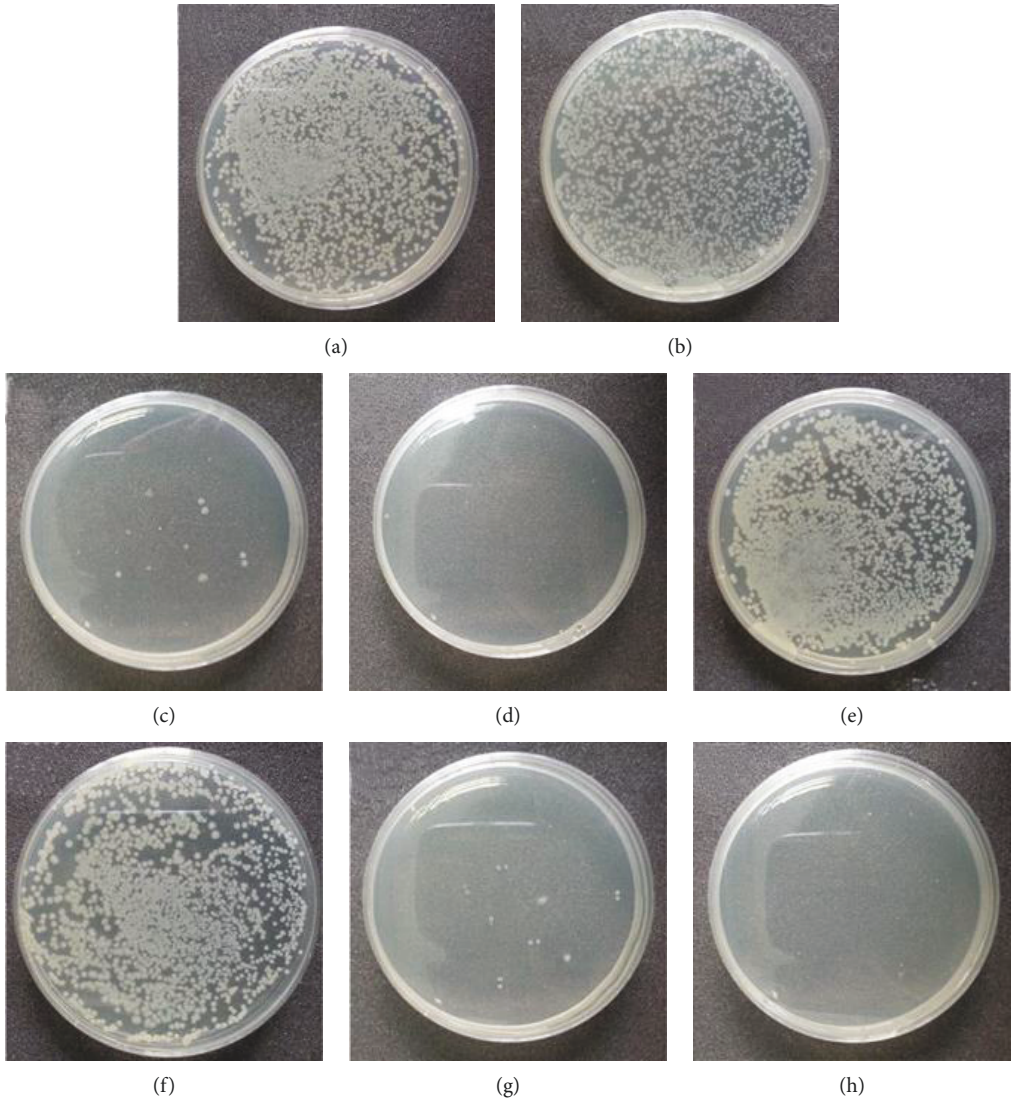

Figure 5: Digital photos of *E. coli* (a, b, c, d) and *S. aureus* (e, f, g, h) colonies after incubation with PBSu (a, e), nLBC (b, f), and cnLBC (c, g) scaffolds and vancomycin (d, h) for 24 hours.

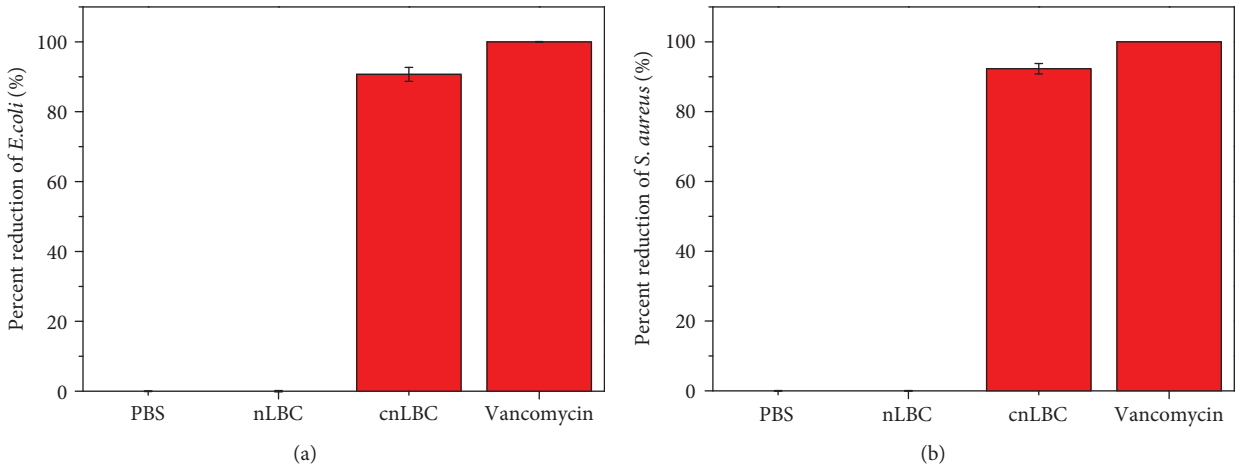

Figure 6: Percent reduction of *E. coil* (a) and *S. aureus* (b) on PBS, nLBC, and cnLBC scaffolds and vancomycin for 24 hours.

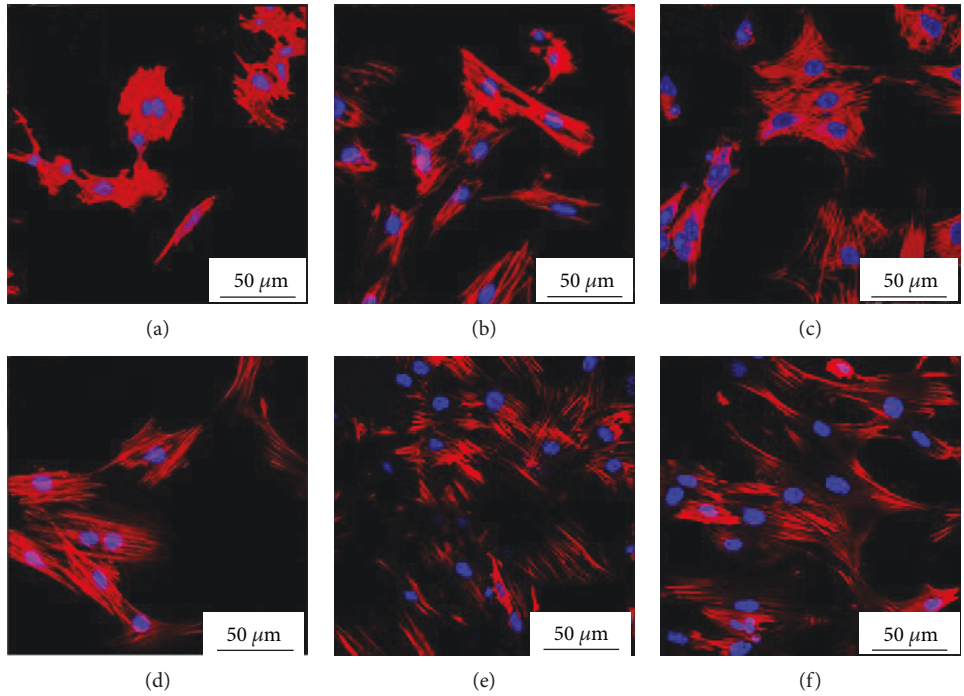

Figure 7: Confocal laser scanning microscopy (CLSM) images of BMSCs on PBS (a, d), nLBC (b, e), and cnLBC (c, f) scaffolds for 1 day (a, b, c) and 3 days (d, e, f).

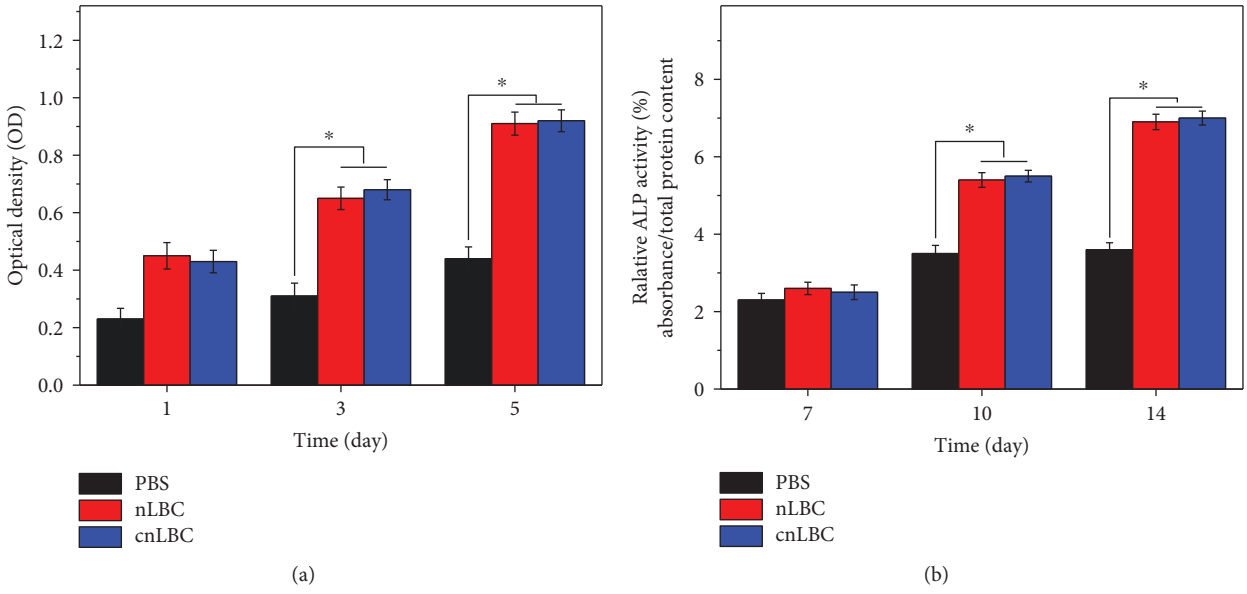

Figure 8: Optical density (OD, a) value and alkaline phosphatase (ALP, b) activity of BMSCs on PBS, nLBC, and cnLBC scaffolds for different times.

4. Discussion

There are increasing demands for biomedical materials to repair bone defects, caused by trauma, infection, congenital diseases, tumor, etc. [22] Promoting bone tissue regeneration and resistance to bacterial infection would be a very desirable property of biomaterials for bone repair [23]. To improve the biological performances (e.g., bioactivity/biocompatibility) and antibacterial activity, cnLAP was coated on PBSu scaffolds with macropore sizes of 300-500 μm by poly(dopamine) modification. After coating with cnLAP, no obvious differences in macroporous structure (e.g., pore morphology and pore size) were found among these PBSu scaffolds, indicating that cnLAP coating did not have significant effects on

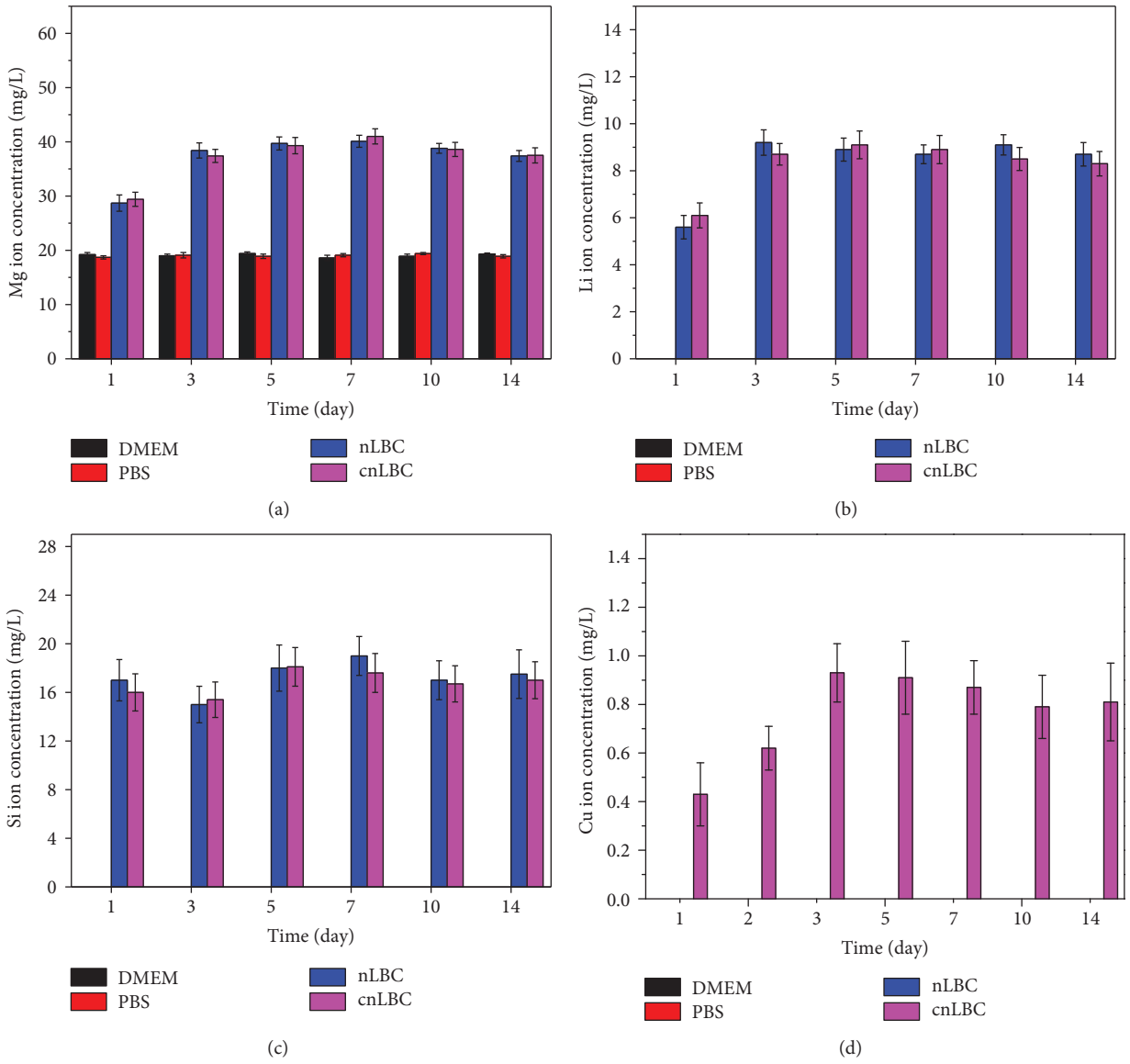

Figure 9: Changes of concentrations of Mg (a), Li (b), Si (c), and Cu (d) ions in cell culture medium with time after BMSCs cultured on PBS, nLBC, and cnLBC scaffolds (DMEM as blank control).

the macroporous structure of PBSu scaffolds. From the SEM, IR, XRD, and XPS analysis, the results indicated that cnLAP was coated on the macroporous surfaces of PBSu scaffolds.

Infection is one of the primary causes of failure of bone implant, and lack of antibacterial activity of the implant surface often causes undesirable complications (e.g., infections) [24]. To treat the infections caused by implants, various antibiotics are adopted [25]. Nevertheless, bacteria could develop drug resistance against multiple antibiotics. Consequently, higher doses of antibiotics are required against drug-resistance bacteria, which eventually results in adverse side effects [26]. Compared with antibiotics, Cu ions have been demonstrated to possess satisfactory antibacterial properties with lower cytotoxicity to the human body [27]. Cu^{2+} is reported to cause dysfunction of the bacterial respiratory enzyme by interacting with the thiol group in the enzyme [28]. Moreover, Cu^{2+} can extract electrons from bacteria, thus destroying the membrane and oxidizing the nuclei of bacteria [28, 29]. In this study, cnLAP was prepared by the cation-exchanged method, and cnLAP coating on the PBSu scaffold was fabricated. The results showed that compared with PBSu and nLBC scaffolds, the cnLBC scaffolds with cnLAP coating could inhibit the growth of both *E. coli* and *S. aureus*, indicating that cnLBC scaffolds possessed good antibacterial activity due to cnLAP-containing Cu ions. Therefore, it is expected that the cnLBC scaffolds would have the ability to resist against bacterial infection when implanted in vivo, which is a very desirable biomaterial property for orthopedic applications.

As a scaffold for bone repair, the biological performances (e.g., bioactivity/biocompatibility) of PBSu scaffolds are very important [30]. In in vitro cell experiments, the results showed that only a few cells attached on PBSu scaffolds while a great number of cells attached on both nLBC and cnLBC

scaffolds, indicating that the coatings of nLAP and cnLAP on PBSu scaffolds significantly promoted the cell adhesion on the scaffolds. Moreover, no significant differences in cell morphology and amount of BMSCs were found on nLBC and cnLBC scaffolds, indicating that incorporation of Cu into nLAP had no negative effects on the cell adhesion. The proliferation of cells on the scaffolds is the second stage of the bone remodeling process after cell adhesion, which determines the following cell differentiation, mineralization, and eventual bone formation [31]. In this study, the results showed that the proliferation of BMSCs on both nLBC and cnLBC were higher than PBSu scaffolds, indicating that coating of nLAP and cnLAP on PBSu scaffolds promoted the cell proliferation. Furthermore, there were no significant differences in cell proliferation in between nLBC and cnLBC scaffolds, revealing that the incorporation of Cu into nLAP had no negative effects on the cell proliferation. ALP is upregulated at the early stage of osteoblast differentiation, and ALP activity is considered an early indicator of osteogenic differentiation, bone formation, and matrix mineralization [32]. In this study, the results showed that the ALP activity of BMSCs cultured on nLBC and cnLBC scaffolds was obviously higher than the PBSu scaffold ($p < 0.05$), indicating that both nLBC and cnLBC scaffolds obviously promoted cell differentiation. Furthermore, there were no significant differences in ALP activity between nLBC and cnLBC scaffolds, revealing that incorporation of Cu into nLAP had no negative effects on cell differentiation.

Previous studies have shown that nLAP could promote cell proliferation and differentiation [8, 10]. In this study, it could be suggested that compared with PBSu scaffolds, the improvement of adhesion, proliferation, and differentiation of BMSCs was ascribed to the presence of coatings of nLAP and cnLAP on nLBC and cnLBC scaffolds. Furthermore, no significant differences in cells' response to both nLBC and cnLBC scaffolds were found. It could be suggested that incorporation of Cu into nLAP had no negative effects on cell behaviors and functions, indicating good cytocompatibility.

Previous studies have shown that suitable concentrations for Mg, Si, and Li ions could stimulate cell adhesion, proliferation, and differentiation. In this study, the results showed that the Mg, Si, and Li ions were gradually released from both nLBC and cnLBC scaffolds into the cell culture medium with time due to the gradual dissolution of both cnLAP and nLAP on the PBSu scaffolds into the medium. In addition, at 14 days, the concentrations for Mg, Si, and Li ions were 106.7, 100.8, and 49.6 mg/L, respectively. Therefore, the promotion of adhesion, proliferation, and differentiation of BMSCs was ascribed to the release of Mg, Si, and Li ions from coating on the scaffolds into the cell culture mediums. Although a high concentration of Cu ions can induce cytotoxicity, it is generally accepted that Cu is safe and cytocompatible at low concentrations (<152 mg/mL) [33]. In this study, Cu ions were found to be gradually released from the cnLBC scaffold into the medium during soaking time, and the concentration of Cu ions was at 4.74 mg/L in the cell culture medium at 14 days. Therefore, the concentration of Cu ions in the cell culture medium was safe. In short, cnLPA coated on PBSu scaffolds has good bioperformances (improved adhesion, proliferation, and differentiation of BMSCs) and antibacterial activity, which might have a great potential for applications in bone tissue engineering.

5. Conclusion

cnLAP was prepared by the cation exchange method, and cnLPA coating on macroporous PBSu scaffolds was fabricated by poly(dopamine) modification. The cnLPA-coated scaffolds exhibited good antibacterial activity, which could inhibit the growth of both *Escherichia coli (E. coli)* and *Staphylococcus aureus (S. aureus)*. Moreover, compared with PBSu scaffolds, both nLAP- and cnLAP-coated PBSu scaffolds significantly improved proliferation and ALP activity of BMSCs. Furthermore, the results demonstrated that incorporation of Cu into nLAP had no negative effects on cells' responses to cnLAP-coated PBSu scaffolds, indicating good cytocompatibility. The results suggested that the cnLAP-coated PBSu scaffolds might offer promising opportunities for promoting bone regeneration and prevention of infectious from bacteria and effective treatment of bone defects.

Data Availability

The data used to support the findings of this study are included within the article.

Conflicts of Interest

The authors declare that they have no conflict of interest.

Acknowledgments

The grants were from the National Natural Science Foundation of China (51772194 and 81771990), Key Medical Program of Science and Technology Development of Shanghai (17441900600, 15441902500), and the Ministry of Education, Youth and Sports of the Czech Republic - Program NPU I (LO1504).

References

[1] Y. Zhang, X. Zhang, C. Zhang et al., "Biodegradable mesoporous calcium–magnesium silicate-polybutylene succinate scaffolds for osseous tissue engineering," *International Journal of Nanomedicine*, vol. 10, 2015.

[2] M. Gigli, M. Fabbri, N. Lotti, R. Gamberini, B. Rimini, and A. Munari, "Poly(butylene succinate)-based polyesters for biomedical applications: a review," *European Polymer Journal*, vol. 75, pp. 431–460, 2016.

[3] M. Nerantzaki, I. Koliakou, M. G. Kaloyianni et al., "A biomimetic approach for enhancing adhesion and osteogenic differentiation of adipose-derived stem cells on poly(butylene succinate) composites with bioactive ceramics and glasses," *European Polymer Journal*, vol. 87, pp. 159–173, 2017.

[4] Z. Y. Wu, K. Zheng, J. Zhang et al., "Effects of magnesium silicate on the mechanical properties, biocompatibility, bioactivity, degradability, and osteogenesis of poly(butylene succinate)-based composite scaffolds for bone repair," *Journal of Materials Chemistry B*, vol. 4, no. 48, pp. 7974–7988, 2016.

[5] M. Ghadiri, H. Hau, W. Chrzanowski, H. Agus, and R. Rohanizadeh, "Laponite clay as a carrier for in situ delivery of tetracycline," *RSC Advances*, vol. 3, no. 43, 2013.

[6] A. A. Thorpe, S. Creasey, C. Sammon, and C. Le Maitre, "Hydroxyapatite nanoparticle injectable hydrogel scaffold to support osteogenic differentiation of human mesenchymal stem cells," *European Cells and Materials*, vol. 32, pp. 1–23, 2016.

[7] K. Li, S. G. Wang, S. H. Wen et al., "Enhanced in vivo antitumor efficacy of doxorubicin encapsulated within laponite nanodisks," *ACS Applied Materials & Interfaces*, vol. 6, no. 15, pp. 12328–12334, 2014.

[8] D. H. Su, L. B. Jiang, X. Chen, J. Dong, and Z. Z. Shao, "Enhancing the gelation and bioactivity of injectable silk fibroin hydrogel with laponite nanoplatelets," *ACS Applied Materials & Interfaces*, vol. 8, no. 15, pp. 9619–9628, 2016.

[9] L. Tao, L. Zhonglong, X. Ming et al., "*In vitro* and *in vivo* studies of a gelatin/carboxymethyl chitosan/LAPONITE® composite scaffold for bone tissue engineering," *RSC Advances*, vol. 7, no. 85, pp. 54100–54110, 2017.

[10] S. Xiao, J. Rodrigues, and H. Tomás, "Laponite-based nanohybrids for enhanced solubility of dexamethasone and osteogenic differentiation of human mesenchymal stem cells," *Journal of Controlled Release*, vol. 259, pp. E121–E122, 2017.

[11] S. Narisawa, M. C. Yadav, and J. L. Millán, "In vivo overexpression of tissue-nonspecific alkaline phosphatase increases skeletal mineralization and affects the phosphorylation status of osteopontin," *Journal of Bone and Mineral Research*, vol. 28, no. 7, pp. 1587–1598, 2013.

[12] W. Zhai, H. Lu, L. Chen et al., "Silicate bioceramics induce angiogenesis during bone regeneration," *Acta Biomaterialia*, vol. 8, no. 1, pp. 341–349, 2012.

[13] H. Sai, L. Xing, J. Xiang et al., "Flexible aerogels with interpenetrating network structure of bacterial cellulose-silica composite from sodium silicate precursor via freeze drying process," *RSC Advances*, vol. 4, no. 57, 2014.

[14] D. Campoccia, L. Montanaro, and C. R. Arciola, "A review of the biomaterials technologies for infection-resistant surfaces," *Biomaterials*, vol. 34, no. 34, pp. 8533–8554, 2013.

[15] H. J. Busscher, H. C. van der Mei, G. Subbiahdoss et al., "Biomaterial-associated infection: locating the finish line in the race for the surface," *Science Translational Medicine*, vol. 4, no. 153, article 153rv10, 2012.

[16] C. Wu, Y. Zhou, M. Xu et al., "Copper-containing mesoporous bioactive glass scaffolds with multifunctional properties of angiogenesis capacity, osteostimulation and antibacterial activity," *Biomaterials*, vol. 34, no. 2, pp. 422–433, 2013.

[17] M. E. S. Achard, S. L. Stafford, N. J. Bokil et al., "Copper redistribution in murine macrophages in response to Salmonella infection," *The Biochemical Journal*, vol. 444, no. 1, pp. 51–57, 2012.

[18] B. Benli and C. Yalin, "The influence of silver and copper ions on the antibacterial activity and local electrical properties of single sepiolite fiber: a conductive atomic force microscopy (C-AFM) study," *Applied Clay Science*, vol. 146, pp. 449–456, 2017.

[19] S. Li, M. Wang, X. Chen, S. F. Li, J. Li-Ling, and H. Q. Xie, "Inhibition of osteogenic differentiation of mesenchymal stem cells by copper supplementation," *Cell Proliferation*, vol. 47, no. 1, pp. 81–90, 2014.

[20] S. Vimalraj, S. Rajalakshmi, D. Raj Preeth et al., "Mixed-ligand copper(II) complex of quercetin regulate osteogenesis and angiogenesis," *Materials Science and Engineering: C*, vol. 83, pp. 187–194, 2018.

[21] S. Zelenay, A. M. Keller, P. G. Whitney et al., "The dendritic cell receptor DNGR-1 controls endocytic handling of necrotic cell antigens to favor cross-priming of CTLs in virus-infected mice," *The Journal of Clinical Investigation*, vol. 122, no. 5, pp. 1615–1627, 2012.

[22] D. Tang, R. S. Tare, L. Y. Yang, D. F. Williams, K. L. Ou, and R. O. C. Oreffo, "Biofabrication of bone tissue: approaches, challenges and translation for bone regeneration," *Biomaterials*, vol. 83, pp. 363–382, 2016.

[23] V. Palmieri, M. Barba, L. di Pietro et al., "Reduction and shaping of graphene-oxide by laser-printing for controlled bone tissue regeneration and bacterial killing," *2D Materials*, vol. 5, no. 1, article 015027, 2017.

[24] D. Li, P. Lv, L. Fan et al., "The immobilization of antibiotic-loaded polymeric coatings on osteoarticular Ti implants for the prevention of bone infections," *Biomaterials Science*, vol. 5, no. 11, pp. 2337–2346, 2017.

[25] E. M. Pritchard, T. Valentin, B. Panilaitis, F. Omenetto, and D. L. Kaplan, "Antibiotic-releasing silk biomaterials for infection prevention and treatment," *Advanced Functional Materials*, vol. 23, no. 7, pp. 854–861, 2013.

[26] R. Singh, L. Sripada, and R. Singh, "Side effects of antibiotics during bacterial infection: mitochondria, the main target in host cell," *Mitochondrion*, vol. 16, no. 14, pp. 50–54, 2014.

[27] T. Xi, M. B. Shahzad, D. Xu et al., "Effect of copper addition on mechanical properties, corrosion resistance and antibacterial property of 316L stainless steel," *Materials Science and Engineering: C*, vol. 71, pp. 1079–1085, 2017.

[28] O. Sharifahmadian, H. R. Salimijazi, M. H. Fathi, J. Mostaghimi, and L. Pershin, "Relationship between surface properties and antibacterial behavior of wire arc spray copper coatings," *Surface and Coating Technology*, vol. 233, pp. 74–79, 2013.

[29] O. Akhavan and E. Ghaderi, "Cu and CuO nanoparticles immobilized by silica thin films as antibacterial materials and photocatalysts," *Surface and Coating Technology*, vol. 205, no. 1, pp. 219–223, 2010.

[30] Y. W. Yoo, G. J. Park, and W. K. Lee, "Surface modification of coralline scaffold for the improvement of biocompatibility and bioactivity of osteoblast," *Journal of Industrial and Engineering Chemistry*, vol. 33, pp. 33–41, 2016.

[31] D. Hong, H. X. Chen, H. Q. Yu et al., "Morphological and proteomic analysis of early stage of osteoblast differentiation in osteoblastic progenitor cells," *Experimental Cell Research*, vol. 316, no. 14, pp. 2291–2300, 2010.

[32] A. Dela Cruz, M. Mattocks, K. S. Sugamori, M. D. Grynpas, and J. Mitchell, "Reduced trabecular bone mass and strength in mice overexpressing Gα11 protein in cells of the osteoblast lineage," *Bone*, vol. 59, pp. 211–222, 2014.

[33] Z. Liu, F. Song, Z. L. Ma et al., "Bivalent copper ions promote fibrillar aggregation of KCTD1 and induce cytotoxicity," *Scientific Reports*, vol. 6, no. 1, article 32658, 2016.